

# Ultrafast photoinduced magnetic moment in a charge-orbital-ordered antiferromagnetic $\text{Nd}_{0.5}\text{Sr}_{0.5}\text{MnO}_3$ thin film

K. Miyasaka,<sup>1</sup> M. Nakamura,<sup>1</sup> Y. Ogimoto,<sup>2</sup> H. Tamaru,<sup>3</sup> and K. Miyano\*<sup>1</sup>Department of Applied Physics, The University of Tokyo, Tokyo 113-8656, Japan<sup>2</sup>Devices Technology Research Laboratories, SHARP Corporation, 2613-1 Tenri, Nara 632-8567, Japan<sup>3</sup>Research Center for Advanced Science and Technology (RCAST), The University of Tokyo, Tokyo 153-8904, Japan<sup>4</sup>PRESTO, Japan Science and Technology Agency, 4-1-8 Honcho Kawaguchi, Saitama 332-0012, Japan

(Received 15 March 2006; revised manuscript received 16 May 2006; published 10 July 2006)

The effect of photoexcitation in the charge sector on the magnetization has been studied with subpicosecond optical pump-and-probe measurements in an antiferromagnetic manganite. Magneto-optic Kerr measurements show a steplike increase of magnetic moment followed by a gradual growth. The steplike behavior is ascribed to the spin flip scattering in the excited states while the slower process to the spin-lattice thermalization, which exhibits slowing down toward the antiferromagnetic-ferromagnetic transition temperature. The time scale of these processes is much faster compared to the photoinduced demagnetization time of ferromagnetic manganites and reflects the effect of underlying spin-charge-orbital order.

DOI: 10.1103/PhysRevB.74.012401

PACS number(s): 75.47.Lx, 78.47.+p

Competition between contrasting phases is one of the most fascinating aspects of the so-called strongly correlated electron systems. It is well exemplified in the phase diagram of an organic superconductor  $(\text{BEDT-TTF})_2X$ , in which a superconducting phase is right next to an insulating phase as a function of the anion  $X$ .<sup>1</sup> Another example is found in manganites. Here, the competing phases are an antiferromagnetic (AFM) insulator and a ferromagnetic (FM) metal. The transition between the two caused by a magnetic field is the so-called colossal magnetoresistance (CMR) of the first kind, CMR1,<sup>2</sup> accompanied by the resistivity jump of more than nine orders of magnitude.<sup>3</sup> Photoinduced insulator-to-metal transition (IMT) has also been reported.<sup>4</sup> In this case, the photoexcitation acts on the charge sector of the insulator, which is in the charge- and orbital-ordered (COO) state as well as in an AFM insulator. The transition is understood in terms of the “melting of a charge solid by light”<sup>5</sup> and the IMT is a natural consequence of it. However, in the spin sector, this is a transition between two ordered phases, an AFM phase and a FM phase. Since the two states both have long-range magnetic order, the emergence of FM order out of the AFM background after the photodestruction of the COO state is a nontrivial question. This is in striking contrast to the much studied photoinduced demagnetization in the FM state, in which the photoexcitation induces disordered paramagnetic (PM) state.<sup>6–9</sup>

Here, we report on the study of the early spin dynamics that eventually leads to the photoinduced AFM-to-FM transition using a subpicosecond pump-and-probe method. Combining the reflectivity and magneto-optic Kerr measurements, we found that the magnetic moment appears in two steps; one occurs within the electron-lattice thermalization time and the other has a characteristic time constant of the order of a few picoseconds showing slowing down toward the AFM-FM transition temperature,  $T_N$ . We believe this is the first observation of the critical nature of the AFM-to-FM transition in a manganite.<sup>10</sup> The nonthermal character of the initial step is in good accord with the recent observation of the photoinduced transition toward the *lower* temperature FM phase.<sup>11</sup>

The measurements were performed on a  $\text{Nd}_{0.5}\text{Sr}_{0.5}\text{MnO}_3$  thin film, which has been grown by a pulsed laser deposition method on a perovskite  $\text{SrTiO}_3(011)$  substrate.<sup>12</sup> The thickness of the film was about 80 nm, which allowed us to excite and probe the whole sample depth without concern about the penetration depth. Figure 1(a) shows the temperature dependence of the magnetization, with  $T_N$  at 160 K and a Curie temperature ( $T_C$ ) at 230 K. The phase sequence is consistent with the temperature dependence of zero-field resistivity [Fig. 1(b)]. Detailed x-ray diffraction study<sup>13</sup> shows that the

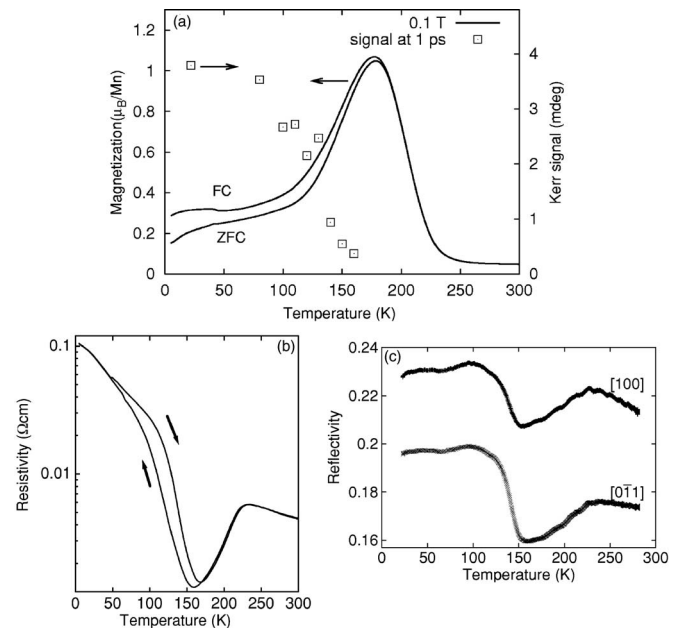


FIG. 1. (a) Temperature dependence of magnetization for  $\text{Nd}_{0.5}\text{Sr}_{0.5}\text{MnO}_3$  (line) and the value of Kerr signal transient at 1 ps (squares). The magnetization was measured with zero-field-cooled (ZFC) and field-cooled (FC) runs applying a magnetic field of 0.1 T along the [100] direction. (b) Temperature dependence of resistivity in a zero magnetic field. (c) Temperature dependence of reflectivity at 800 nm using the same experimental setup as that of time-resolved measurements. Labels indicate the polarization directions.

orbital order appears below  $T_N$  followed by the charge order at slightly lower temperature. The COO state is consistent with a modified CE-type AFM state in marked contrast to the A-type AFM of bulk single crystals.<sup>14</sup> We therefore assume that the spin arrangement is similar to that of the CE-type AFM with a slight canting resulting in the net magnetization [Fig. 1(a)]. The COO plane normal is along [001], tilted at 45° from the film surface. This is in accord with the temperature dependence of the anisotropic reflectivity measured at 800 nm shown in Fig. 1(c). The sharper change for the polarization along  $[0\bar{1}1]$  (probing half intraplane and half interplane contributions) compared with that along [100] (totally intra-plane) at the COO AFM-to-FM boundary reflects the two-dimensional (2D) character of the electronic state of the COO state. The transfer integral between the Mn atoms within the COO plane is much enhanced compared with that across the planes.

The optical time-resolved measurements were performed using a Ti:sapphire regenerative amplifier system with a pulse width of 150 fs and a repetition rate of 1 kHz in the reflection mode. The pump wavelengths of 800 nm and 400 nm were employed, with no qualitative difference between the two in the ultrafast transients. The reflectivity was probed either at 800 nm or 400 nm. The magnetization dynamics were measured with the polar Kerr configuration in a magnetic field of 0.2 T applied perpendicularly to the surface. In order to eliminate the contribution of photoinduced optical anisotropy due to the background birefringence of nonmagnetic origin, the Kerr signal was recorded by taking the difference in the polarization change in the opposite magnetic field directions normalized with the reflectivity.

The essential features of the photoinduced magnetic moment in the COO-AFM state are captured in Fig. 2. Figure 2(a) shows transient magneto-optic Kerr rotation probed by 400 nm [100] polarized light at 22 K. Photoexcitation brings a sudden increase of Kerr rotation in 1 ps (process 0, dotted line). After the fast increase, the Kerr signal exhibits little change over 10 ps and then shows an oscillation. The oscillation is a precession of the net moment present in the AFM state before the photoexcitation [Fig. 1(a)]. Because the photoexcitation induces a sudden change in magnetic anisotropy, the spins start to precess (process 2).<sup>15,16</sup> There is another component in the Kerr signal: a slowly rising magnetization with a few ps time scale (process 1) shown in dashed line in Fig. 2(a). The observed response in the initial 10 ps is the superposition of process 1 and a negatively going half cycle of the precession, which is more clearly seen in Fig. 4.

With the reflectivity and Kerr data combined, we can now discuss the entire photoexcitation process.

*Process 0* ( $\leq 1$  ps). The transient reflectivity change [Fig. 2(d)] shows that, both in [100] and  $[0\bar{1}1]$  directions, the photoexcitation induces a sharp decrease of reflectivity in less than 0.5 ps followed by a fast increase in 1.3 ps. The CT transition is dominant in the photoexcitation of the COO-AFM state favoring metallic extended states with isotropic interaction (charge- and orbital-disordered state). The initial dip is due to the population of these states. We ascribe the subsequent reflectivity increase to the electron-lattice thermalization, which has been known to have a time constant of

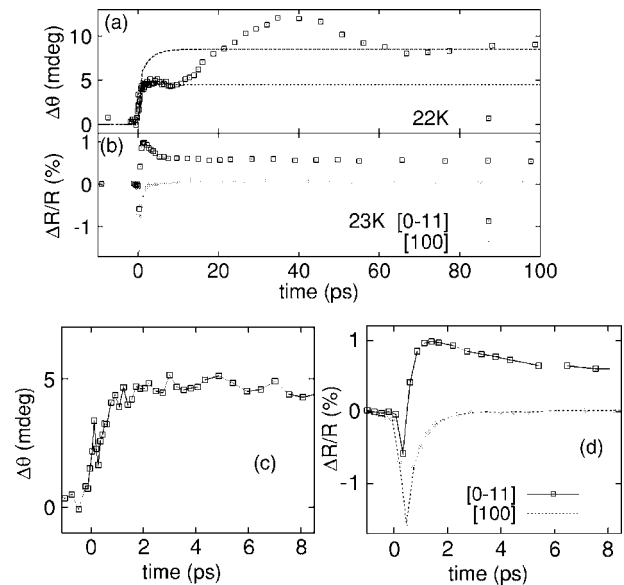


FIG. 2. (a) Transient Kerr rotation  $\Delta\theta(t)$  probed by [100] polarized 400 nm light pulses at 22 K. The pump intensity was  $600 \mu\text{J}/\text{cm}^2$  and the wavelength 800 nm. (b) Transient reflectivity  $\Delta R(t)/R$  probed by 800 nm light pulses at 23 K. The pump intensity was  $220 \mu\text{J}/\text{cm}^2$  and the wavelength 800 nm. (c) and (d) The expanded views of (a) and (b), respectively.

the order of 1 ps both in metals<sup>17</sup> and in manganites.<sup>18</sup> Following the scenario proposed by Beaupaire *et al.*,<sup>19</sup> a sub picosecond emergence of the magnetization is naturally understood in terms of the spin-flip scattering while the electrons are in the photoexcited states through the spin-orbit interaction.<sup>20</sup> The delocalized excited states favor parallel spin alignment via the double exchange mechanism (DEM). This corresponds to the steplike increase in the Kerr signal in Fig. 2(a). Note that the smooth Kerr signal change in the expanded view [Fig. 2(c)] indicates that the coherent spin-flip mechanism<sup>21</sup> is not at work here. The magnetic moment is still small [the step in Fig. 2(a) corresponds to  $0.015 \mu_B/\text{Mn}$ ], and the spin temperature has to reach the electron-lattice temperature.

*Process 1* (between 1 ps and 10 ps). Here the dynamics probed by the light polarized along [100] and  $[0\bar{1}1]$  are different [Figs. 2(b) and 2(d)]. In the  $[0\bar{1}1]$  direction, there is a decay, which is absent in the [100] direction. The anisotropic behavior reflects the underlying electronic anisotropy of the COO-AFM phase (interplane vs intraplane). With a stronger intra-plane interaction along the [100] direction to start with, the effect of the photoexcitation is naturally smaller. Therefore, the reflectivity transient along the [100] direction completes after the electron and lattice are thermalized. On the other hand, the transfer integral between the Mn atoms on neighboring planes is initially suppressed due to the interplane AFM spin arrangement. As the spins align between the planes, both the magnetization [Fig. 2(a), dashed line] and interplane interaction [Fig. 2(b), upper trace] grow hand in hand via DEM. This is the initial stage of the AFM to FM transition after the electron-lattice thermalization, which should be compared to the slow demagnetization process in

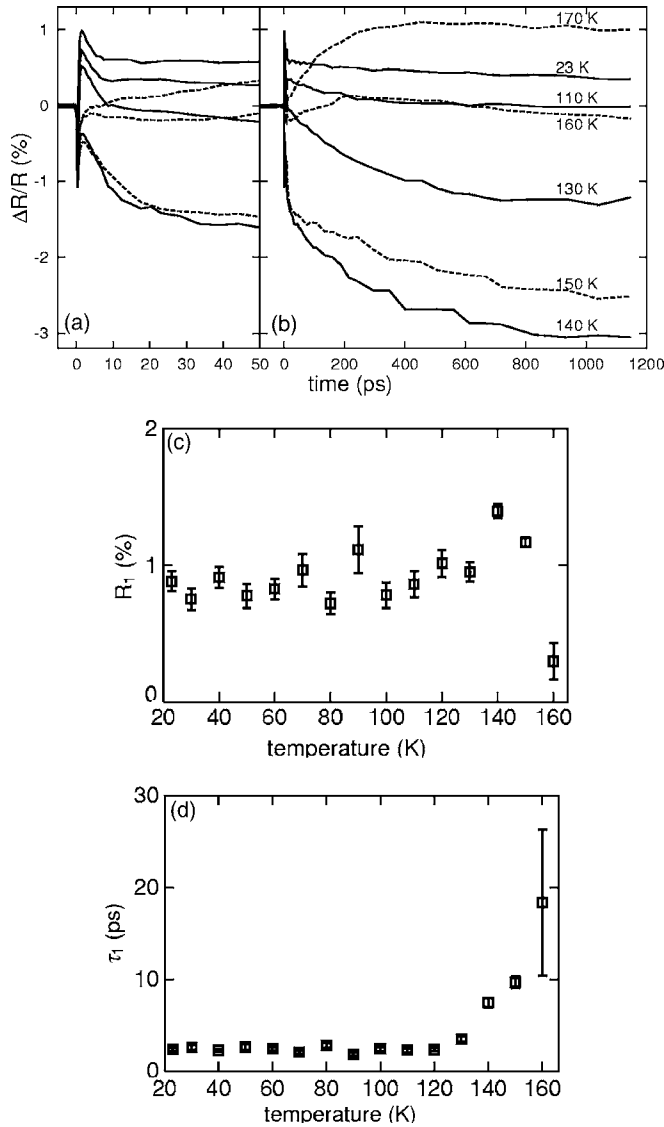


FIG. 3. Photoinduced reflectivity transients probed by  $[0\bar{1}1]$  polarized 800 nm pulses in (a) short- and (b) long-time range. The temperature is labeled for each curve in (b). (c) and (d) show the results of fittings using the empirical two exponentials. (c) represents amplitude and (d) time constant for process 1.

FM manganites.<sup>6</sup> The difference in the time constant, a few picoseconds vs hundreds of picoseconds, is striking. The two transients, the Kerr signal and the reflectivity, have the same time constant. This is the case at all temperatures as long as the fast rising Kerr signal is clearly discerned (see Figs. 3 and 4). While the reflectivity transients depend on the polarization, the results of Kerr measurement are independent of the probe polarization. This ensures that the influence of the reflectivity transients (a much stronger feature in the raw data) is negligible in our measurement and the Kerr signal faithfully indicates the magnetic state.

The photoinduced magnetism was kept small here in order to avoid getting into a long-lived metastable FM state, whose extreme case is the persistent transition.<sup>11</sup> Below the pump power density employed here ( $\leq 1$  mJ/cm<sup>2</sup>), the effect was linear to the pump power. However, as the power den-

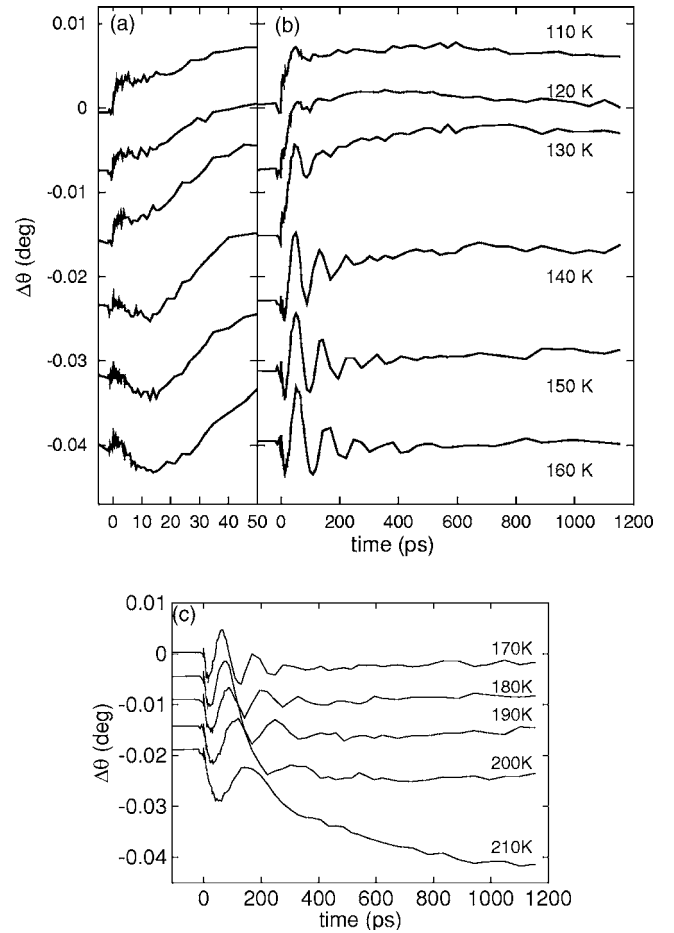


FIG. 4. Temperature dependence of photoinduced magneto-optical Kerr rotation transients. The transients in (a) short- and (b) long-time range below  $T_N$ . (c) Temperature dependence of the Kerr signal in the ferromagnetic temperature range.

sity increased ( $\geq 2.0$  mJ/cm<sup>2</sup>), a qualitatively different response appeared: the Kerr signal suddenly gets much larger and slower while the reflectivity tends to saturate. This may signal the emergence of the real coherent FM order. At this stage, however, the data are not reliable because the effect of the long-lived component cannot be estimated in pump-and-probe measurements anymore. Since we are interested in the incipient processes right after the photoexcitation, we are obliged to stay in the low power limit.

We now concentrate on the temperature dependence. Figure 3 shows the normalized reflectivity transients along  $[0\bar{1}1]$  mainly in the AFM temperature range,  $T \leq 170$  K. We fitted the temporal behavior using a superposition of two exponentials,  $\Delta R(t)/R = R_0 + R_1 \exp(-t/\tau_1) + R_2 \exp(-t/\tau_2)$ . The fast relaxation [Fig. 3(a), corresponding to process 1] gets slower toward  $T_N$  [Fig. 3(d)] and then disappears above it [Fig. 3(c)]. This behavior is quite reasonable considering the weakening of the interplane AFM coupling toward the transition point and its absence above  $T_N$ .

The long-time dynamics presented in Fig. 3(b) show relaxations of hundreds of picoseconds. This is the characteristic time scale associated with the FM order.<sup>7-9</sup> The slow relaxation is due to the half-metallicity of the FM state, in

which the spin state is protected against the flip; there are no low-lying reversed spin states into which electrons can scatter. We thus ascribe this slow component to the change of the FM order. The negative reflectivity change in the AFM temperature range and the positive variation in the FM temperature range ( $T=170$  K) are consistent with the growth of FM order in the former case and the demagnetization in the latter case toward the respective thermal equilibrium [see Fig. 1(c)]. The reflectivity change  $\Delta R$  at 1 ns matches well with the derivative of  $R$  with respect to the temperature.  $(dR/dT) \cdot \Delta T$ , meaning that after 1 ns, the system is thermalized completely. The temperature rise  $\Delta T$  is 10 K at  $1 \text{ mJ/cm}^2$ .

Figure 4 represents temperature dependence of photoinduced Kerr rotation transients near  $T_N$ . The transients in short-time range, presented in Fig. 4(a), show that the step like fast response (process 0) as well as the subsequent growth (process 1) decrease as the temperature increases: the latter is eventually eaten up by the negative going cycle of the precession, whose phase is independent of the temperature while its amplitude grows toward  $T_N$ . The step height in process 0 should be proportional to the degree of the AFM order before the laser irradiation because it is a measure of the number of spins that can be flipped while the electrons are in the delocalized states. The degree of AFM order can be estimated from the reduction of magnetization as the temperature is lowered below  $T_N$ . As shown in Fig. 1(a), the step height is the mirror image of the magnetization supporting our proposal that process 0 is the direct generation of parallel magnetic alignment out of AFM ground state.

Figure 4(b) shows the Kerr transients in longer time range. The amplitude of oscillation becomes larger as the temperature increases as a consequence of the increase of the net moment in the AFM state toward  $T_N$  [see Fig. 1(a)].

In the FM temperature range presented in Fig. 4(c), the Kerr signal behaves just as previously reported.<sup>6</sup> It is characterized by a slow decay that lasts for hundreds of picosec-

onds. The demagnetization time constant showed peak near 220 K, which is lower than  $T_C$ . The period of the precession increases at the same time. The period largely depends on the strength of the effective magnetic field which includes external field, demagnetization field, and magnetic anisotropy. The increase of the period implies that the magnetic anisotropy is weakened toward  $T_C$ . The closeness of the features found here to those observed in bulk crystals ensures that there is nothing unusual in thin film samples; especially the different stress state inevitable in thin films does not alter the spin dynamics. Therefore, the results presented here in the AFM state should be applicable to bulk monodomain single crystals as well. The effects of photoexcitation on the COO-AFM phase have been studied in bulk single crystals.<sup>18,22</sup> A fast destruction of the COO after photoexcitation is observed, whose time constant compares well with that of process 0. However, no response corresponding to process 1 has been noticed previously, not to mention the behavior of the magnetic order. It is to be noted that a clear signature of this process is enhanced in the  $[0\bar{1}1]$  polarization, the anisotropic behavior probed for the first time in this study.

In conclusion, photoexcitation of the COO-AFM state aligns the magnetic moment in 1 ps followed by disordering of AFM spins which generates further magnetic moments in the few picoseconds time scale. Photoinduced reflectivity transients suggest critical slowing down. Combining photoinduced reflectivity and magneto-optic Kerr rotation transients, we clearly demonstrate the inherent competition between AFM and FM order.

This work was supported by TOKUTEI Grant No. (16076207) from the MEXT, Japan and JSPS KAKENHI Grant No. (15104006). Financial support to M.N. by the 21st Century COE Program for "Applied Physics on Strong Correlation," administered by the Department of Applied Physics, The University of Tokyo, is also appreciated. The work by Y.O. has been done at the University of Tokyo, on a leave of absence from SHARP Corp.

\*Email address: miyano@myn.rcast.u-tokyo.ac.jp

<sup>1</sup>K. Kanoda, *Physica C* **282**, 299 (1997).

<sup>2</sup>H. Aliaga *et al.*, *Phys. Rev. B* **68**, 104405 (2003).

<sup>3</sup>Y. Tomioka *et al.*, *J. Phys. Soc. Jpn.* **64**, 3626 (1995).

<sup>4</sup>K. Miyano *et al.*, *Phys. Rev. Lett.* **78**, 4257 (1997); M. Fiebig *et al.*, *Science* **280**, 1925 (1998).

<sup>5</sup>Y. Tokura and N. Nagaosa, *Science* **288**, 462 (2000).

<sup>6</sup>T. Ogasawara *et al.*, *Phys. Rev. B* **68**, 180407(R) (2003).

<sup>7</sup>A. I. Lobad *et al.*, *Appl. Phys. Lett.* **77**, 4025 (2000); A. I. Lobad *et al.*, *Phys. Rev. B* **63**, 060410(R) (2001).

<sup>8</sup>J. Wang *et al.*, *Phys. Rev. Lett.* **95**, 167401 (2005).

<sup>9</sup>R. D. Averitt *et al.*, *Phys. Rev. Lett.* **87**, 017401 (2001).

<sup>10</sup>We are aware of one pump-and-probe measurement at the AFM-to-FM transition in a metal, but it should be noted that no mechanism of electron correlation seems to be in effect in this case. See J. U. Thiele *et al.*, *Appl. Phys. Lett.* **85**, 2857 (2004) and G. Ju *et al.*, *Phys. Rev. Lett.* **93**, 197403 (2004). An experiment acting directly on the spin sector by light has been reported recently. See A. V. Kimel *et al.*, *Nature (London)* **435**, 655 (2005).

<sup>11</sup>N. Takubo *et al.*, *Phys. Rev. Lett.* **95**, 017404 (2005).

<sup>12</sup>Y. Ogimoto *et al.*, *Phys. Rev. B* **71**, 060403(R) (2005); M. Nakamura *et al.*, *Appl. Phys. Lett.* **86**, 182504 (2005).

<sup>13</sup>Y. Wakabayashi *et al.*, *Phys. Rev. Lett.* **96**, 017202 (2006).

<sup>14</sup>H. Kawano-Furukawa *et al.*, *Phys. Rev. B* **67**, 174422 (2003).

<sup>15</sup>M. van Kampen *et al.*, *Phys. Rev. Lett.* **88**, 227201 (2002).

<sup>16</sup>The magnetic anisotropy is due probably to the magneto-crystalline anisotropy rather than the demagnetization field. This is because the behavior of the precession does not vary throughout the entire temperature range. The laser-induced demagnetization change can be negative or positive depending on the initial magnetic state.

<sup>17</sup>L. Guidoni *et al.*, *Phys. Rev. Lett.* **89**, 017401 (2002).

<sup>18</sup>T. Ogawara *et al.*, *J. Phys. Soc. Jpn.* **71**, 2380 (2002).

<sup>19</sup>E. Beaurepaire *et al.*, *Phys. Rev. B* **58**, 12134 (1998).

<sup>20</sup>See, for example, T. Ogasawara *et al.*, *Phys. Rev. Lett.* **94**, 087202 (2005) for the strength of the spin-orbit interaction.

<sup>21</sup>W. Hübner and G. P. Zhang, *Phys. Rev. B* **58**, R5920 (1998); R. Gómez-Abal *et al.*, *Phys. Rev. Lett.* **92**, 227402 (2004).

<sup>22</sup>T. Ogasawara *et al.*, *Phys. Rev. B* **63**, 113105 (2001).